

## Synthesis and Photocatalytic Activity of TiO<sub>2</sub>-ZrO<sub>2</sub> Nano-Sized Powders by Sol-Gel Process

Jae-Kil Han, Fumio Saito,\* Jong-Gu Park,\*\* and Byong-Taek Lee<sup>†</sup>

School of Advanced Materials Engineering, Kongju National University, Chungnam 314-701, Korea

\*Institute of Multidisciplinary Research for Advanced Materials, Tohoku University, Sendai 980-8577, Japan

\*\*Nano Materials Technology Center, Korea Institute of Science and Technology, Seoul 136-791, Korea

(Received September 17, 2004; Accepted December 10, 2004)

### ABSTRACT

TiO<sub>2</sub>-ZrO<sub>2</sub> powders were successfully synthesized by the sol-gel process using titanium iso-propoxide as a precursor. The amorphous TiO<sub>2</sub> particles, 70 nm in size, homogeneously adhered to the surface of ZrO<sub>2</sub> the powders. After calcination at 450°C, most of the TiO<sub>2</sub> powders appeared as an anatase type, whereas they changed to a rutile phase at 750°C. For comparison of photocatalytic activity, TiO<sub>2</sub>-ZrO<sub>2</sub> nano-sized powders calcined at 450°C, 600°C, and 750°C were used. In the TiO<sub>2</sub>-20 wt%ZrO<sub>2</sub> powders calcined at 450°C, there was excellent removal efficiency of Methyl Orange (MO). For the calcination temperature increased, TiO<sub>2</sub>-ZrO<sub>2</sub> nano-sized powders increased ZrO<sub>2</sub> contents showed the good photoactivity for the photooxidation of MO.

**Key words :** Nanocrystalline, TiO<sub>2</sub>-ZrO<sub>2</sub> nano-sized powders, Methyl orange, Photocatalytic activity, Sol-gel method

### 1. Introduction

Titanium dioxide (TiO<sub>2</sub>) has used widely in environmental fields because of its intrinsic properties such as strong oxidizing power, nontoxicity, non-energy consuming and long-term photostability.<sup>1-6)</sup> In order to improve photocatalytic activity, additives such as V<sub>2</sub>O<sub>5</sub>, WO<sub>3</sub>, CdS, and SnO<sub>2</sub> were added to the TiO<sub>2</sub> phase.<sup>7-10)</sup> These oxides can be acted on as a Lewis acid because they can easily generate the photon. Thus, the dispersion of above the oxide ceramics in the TiO<sub>2</sub> increases the efficiency of photocatalytic activity.<sup>9)</sup> However, they have some disadvantages for application due to their poor thermal stability and phase transformation at high temperatures. Therefore, many studies have focused on the development of thermal resistance catalysts using secondary phase. ZrO<sub>2</sub> is an especially good candidate material as a secondary phase because of its good mechanical properties, chemical inertia, corrosion resistance and high temperature stability.

Photocatalytic activity depends on the mole ratio of each particle, thermal treatment conditions, the crystalline size and the specific surface area. The effect of crystalline size is especially significant appearing in the purification of pollutants in water, and the optimum particle size was measured to be less than 20 nm the depending on the experimental conditions. Therefore, the properties of catalyst were closely related to the fabrication methods including flame oxida-

tion,<sup>11)</sup> co-precipitation,<sup>12)</sup> chemical vapor deposition,<sup>13)</sup> and the sol-gel process.<sup>14-16)</sup> Among them, the sol-gel process is considered as a good approach for the synthesis of ultra fine powders because it can easily control the solid solution with a stoichiometry and a homogeneous distribution of all components.<sup>16,17)</sup> In particular, the morphology and crystallization of TiO<sub>2</sub> particles is closely related to the calcination conditions such as temperature and duration of time.

In this study, using the sol-gel process, TiO<sub>2</sub>-ZrO<sub>2</sub> nano-sized powders were synthesized to study the retardation effect of anatase-to-rutile phase transformation depending on the ZrO<sub>2</sub> content and calcination temperatures. And also, the performance of Methyl Orange (MO) degradation was investigated using the UV-visible spectroscopy.

### 2. Experimental Procedure

TiO<sub>2</sub>(1- $\chi$ )- $\chi$ ZrO<sub>2</sub> ( $\chi$  = 0.2, 0.4, 0.6, and 0.8) nano-sized powders were synthesized using the sol-gel method with titanium iso-propoxide (Aldrich chemical, 99%) and ZrO<sub>2</sub> nano powders (Tosoh Co., Japan). Detailed synthesis process was followed by paper.<sup>18)</sup> Synthesized TiO<sub>2</sub>(1- $\chi$ )- $\chi$ ZrO<sub>2</sub> nano-sized powders were calcined at 450°C, 600°C, and 750°C for one hour in air.

The crystal structures of TiO<sub>2</sub>-ZrO<sub>2</sub> nano-sized powders were identified by X-ray diffraction (D/MAX250, Rigaku) with CuK $\alpha$  radiation ( $\lambda$  = 1.54056 Å). The morphology and microstructures of TiO<sub>2</sub>-ZrO<sub>2</sub> composite powders were studied using TEM (JEM-2010, Jeol).

To investigate the efficiency of removal of Methyl Orange (MO), 0.2 wt% of TiO<sub>2</sub>-ZrO<sub>2</sub> composite powders were dispersed in an aqueous solution in a pyrex beaker. As an UV

<sup>†</sup>Corresponding author : Byong-Taek Lee

E-mail : lbt@kongju.ac.kr

Tel : +82-41-850-8677 Fax : +82-41-858-2939

irradiation source, 40 W medium-pressure mercury lamp was used. To determine the residual concentration change of MO during UV irradiation, small amounts of solution taken from the reaction solution were analyzed by UV-visible spectrometer. An UV-visible spectrometer (HP8453, Hewlett Packard) was used to measure the absorbance of MO within a range from 200 nm to 700 nm and determine simultaneously the concentration of MO at the maximum wavelength of 465 nm using a 3-point calibration curve.

### 3. Results and Discussion

#### 3.1. Characterization of $\text{TiO}_2$ - $\text{ZrO}_2$ Composite Powders

Fig. 1 shows the typical TEM images of the as-received  $\text{TiO}_2$ -20 wt% $\text{ZrO}_2$  and  $\text{TiO}_2$ -80 wt% $\text{ZrO}_2$  nano-sized powders. On the agglomerated particles, the  $\text{TiO}_2$  particles adhered to the  $\text{ZrO}_2$  surface having a spherical shape. The  $\text{ZrO}_2$  particles show a dark contrast and are about 70 nm in diameter while the  $\text{TiO}_2$  is about 20 nm in diameter. In the TEM images, we can see that the dark contrast increases as the

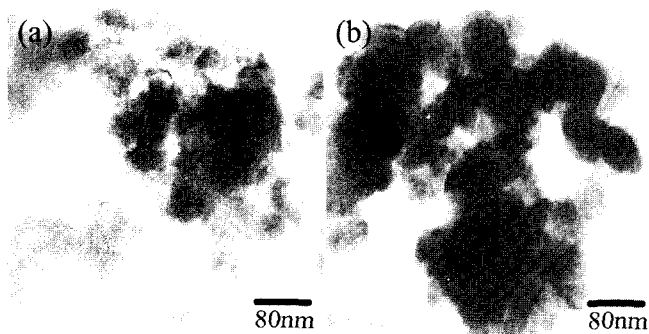


**Fig. 1.** TEM micrographs of as-received  $\text{TiO}_2$ - $\text{ZrO}_2$  composite powders depending on the  $\text{TiO}_2$  contents; (a)  $\text{TiO}_2$ -20 wt% $\text{ZrO}_2$  and (b)  $\text{TiO}_2$ -80 wt% $\text{ZrO}_2$ .

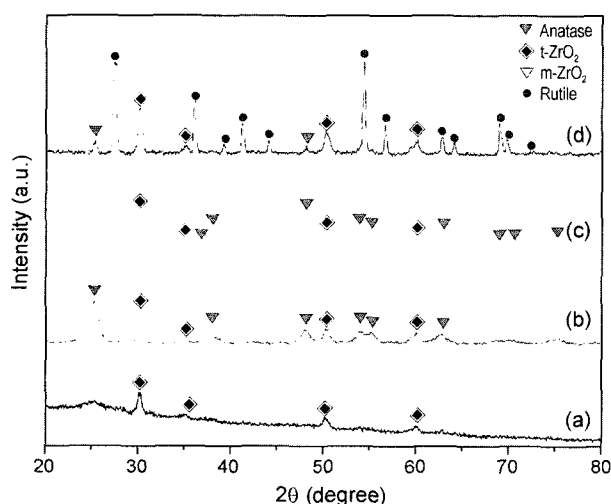


**Fig. 2.** XRD patterns of  $\text{TiO}_2$ -20 wt% $\text{ZrO}_2$  composite powders calcined at (a) as-received, (b) 450°C, (c) 600°C, and (d) 750°C.

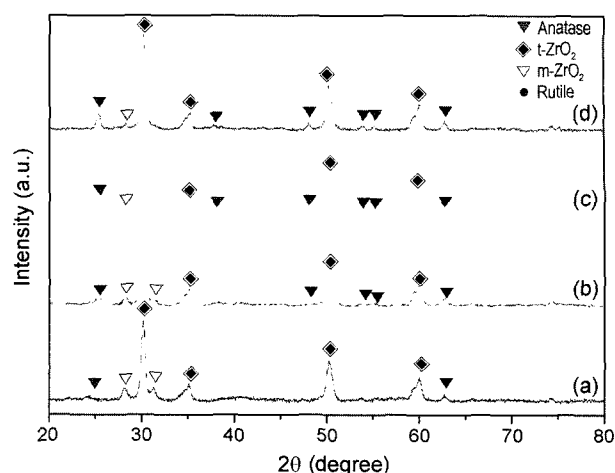


**Fig. 3.** XRD patterns of  $\text{TiO}_2$ -80 wt% $\text{ZrO}_2$  composite powders calcined at (a) as-received, (b) 450°C, (c) 600°C, and (d) 750°C.

$\text{ZrO}_2$  content increases. Also, the aggregation of  $\text{TiO}_2$  particles remarkably increases as the  $\text{TiO}_2$  content increases.

Fig. 2 shows the XRD patterns of as-received  $\text{TiO}_2$ -20 wt%  $\text{ZrO}_2$  nano-sized powders depending on the calcination temperatures.  $\text{ZrO}_2$  powders existed with a tetragonal structure while  $\text{TiO}_2$  was an amorphous phase as indicated in Fig. 2(a). The amorphous  $\text{TiO}_2$  powders were crystallized with an anatase type at 450°C (Fig. 2(b)), and they still existed without any phase transformation although there was some change of sharp peaks, while the anatase structure of  $\text{TiO}_2$  was transformed to the rutile type at 750°C (Fig. 2(d)). In the case of the  $\text{TiO}_2$ -40 wt% $\text{ZrO}_2$ ,  $\text{TiO}_2$ -60 wt% $\text{ZrO}_2$  and  $\text{TiO}_2$ -80 wt% $\text{ZrO}_2$  nano-sized powders, as the  $\text{ZrO}_2$  content increases, the peak intensity of the rutile remarkably decreases at the calcination temperature of 750°C while anatase peaks were strong. However, in Fig. 3(d), the anatase peaks were only detected without rutile peaks. This result indicates that when the anatase  $\text{TiO}_2$  is transformed to the rutile type, there is a critical particle size of  $\text{TiO}_2$ ; i.e., in the  $\text{TiO}_2$ -20 wt% $\text{ZrO}_2$  nano-sized powders, the abundant content of  $\text{TiO}_2$  attached on the  $\text{ZrO}_2$  can be easily grown to a very large size to decrease the surface energy as the of calcination temperature increases, while with the  $\text{TiO}_2$ -80 wt%  $\text{ZrO}_2$  composite powders, the  $\text{TiO}_2$  particles exist separately without agglomeration due to the small amount of  $\text{TiO}_2$ . As a result, it can be understood that  $\text{ZrO}_2$  nano-sized particles act as a stabilizer of the anatase-to-rutile phase transformation of  $\text{TiO}_2$ .

#### 3.2. Photodegradation of Methyl Orange

Fig. 4 shows the absorption spectra of Methyl Orange (MO, 25 ppm) depending on the irradiation time in an aqueous solution, in which  $\text{TiO}_2$ -20 wt% $\text{ZrO}_2$  nano-sized powders calcined at 450°C were dispersed. The wavelength peak of MO showed the primary absorbance at 465 nm. The secondary absorption peak was detected at 271 nm which indicates the phenyl group. The maximum peak indicates that sub-

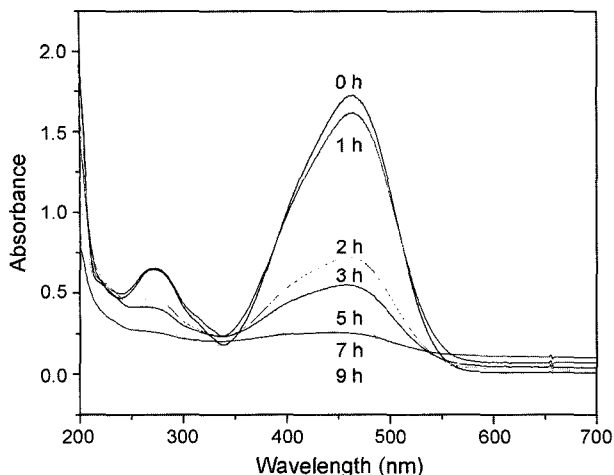


Fig. 4. The UV-visible absorption spectra of methyl orange depending on the irradiation times.

stituents such as the azo, amine and sulfonyl groups can produce a new electron transfer band.<sup>19)</sup> An Hg lamp ranging from 250 to 390 nm in wavelength was used as an UV light source. The absorbance of MO decreased as increase the UV irradiation time increased. After 9 h of UV irradiation, the baseline of MO was a flat. From the result, it can be understood that the substituents of benzene and MO were decomposed efficiently by the photocatalytic activity of TiO<sub>2</sub>-ZrO<sub>2</sub> nano-sized powders.

Fig. 5 shows the performances of MO decomposition in the TiO<sub>2</sub>-ZrO<sub>2</sub> nano-sized powders calcined at 450°C. In the case of TiO<sub>2</sub>-20 wt% ZrO<sub>2</sub> and TiO<sub>2</sub>-40 wt%ZrO<sub>2</sub> composite powders, the removal efficiency of MO showed a similar pattern; i.e, the arrival time for the half value of initial concentration took about 2 h and then the MO concentration reached about 0% after 10 h. On the other hand, the removal efficiency of TiO<sub>2</sub>-60 wt%ZrO<sub>2</sub> and TiO<sub>2</sub>-80 wt%ZrO<sub>2</sub> powders was lower than that of TiO<sub>2</sub>-40 wt%ZrO<sub>2</sub> nano-sized powders. After UV irradiation for 10 h, the residual concentration of MO in the TiO<sub>2</sub>-60 wt%ZrO<sub>2</sub> and TiO<sub>2</sub>-80 wt%ZrO<sub>2</sub>

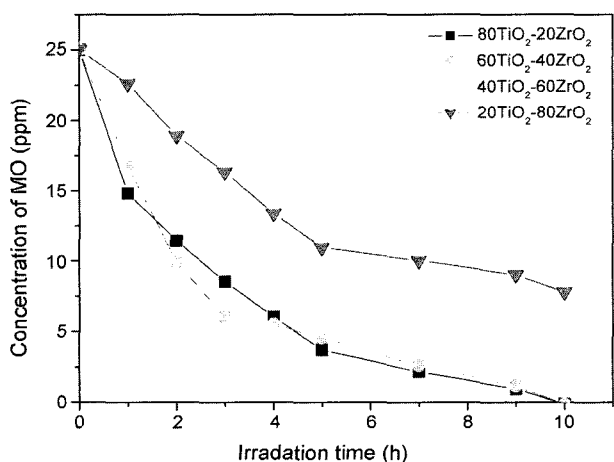


Fig. 5. The performances for MO decomposition compared with TiO<sub>2</sub>-ZrO<sub>2</sub> composite powders calcined at 450°C.

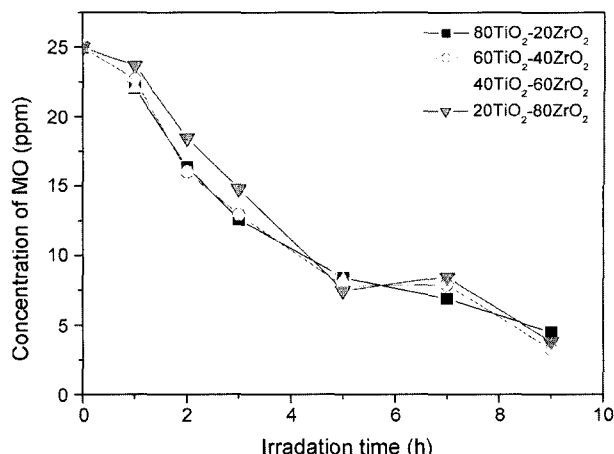


Fig. 6. The performances for MO decomposition compared with TiO<sub>2</sub>-ZrO<sub>2</sub> composite powders calcined at 750°C.

nano-sized powders were 5.5 ppm and 7.8 ppm, respectively. This result indicated that removal efficiency increased as the anatase content increased. Also, from the results of similar removal efficiency in the TiO<sub>2</sub>-40 wt% ZrO<sub>2</sub> and TiO<sub>2</sub>-20 wt%ZrO<sub>2</sub> nano-sized powders, TiO<sub>2</sub>-40 wt%ZrO<sub>2</sub> nano-sized powders showing high intensity of anatase peaks is recommended to decompose organic materials.

Fig. 6 shows the performance of MO degradation in the TiO<sub>2</sub>-ZrO<sub>2</sub> nano-sized powders calcined at 750°C. Without dependence on TiO<sub>2</sub> concentration, they showed the same tendency. However, the efficiency of the TiO<sub>2</sub>-20 wt%ZrO<sub>2</sub> and TiO<sub>2</sub>-40 wt%ZrO<sub>2</sub> nano-sized powders was remarkably lower than when calcined at 450°C as shown in Fig. 5. Thus, after 9 h of UV irradiation, the residual concentrations of MO in the TiO<sub>2</sub>-20 wt%ZrO<sub>2</sub> and TiO<sub>2</sub>-40 wt%ZrO<sub>2</sub> were 4.46 ppm and 3.25 ppm, respectively.

After 9 h of UV irradiation, the residue concentrations of MO determine 4.46 ppm for 80 wt%TiO<sub>2</sub>-ZrO<sub>2</sub>, 3.25 ppm for 60 wt%TiO<sub>2</sub>-ZrO<sub>2</sub>, 2.26 ppm for 40 wt%TiO<sub>2</sub>-ZrO<sub>2</sub>, and 3.78 ppm for 20 wt%TiO<sub>2</sub>-ZrO<sub>2</sub>, respectively. They have increased the degradation rates in the following order: 40 wt%TiO<sub>2</sub>-ZrO<sub>2</sub> > 60 wt%TiO<sub>2</sub>-ZrO<sub>2</sub> > 20 wt%TiO<sub>2</sub>-ZrO<sub>2</sub> > 80 wt%TiO<sub>2</sub>-ZrO<sub>2</sub>. As a result, we can analogize that the removal efficiency is related with the state of phase transformation (anatase → rutile). The quantitative analysis of anatase was calculated with Spur and Mayers relation equation.<sup>20)</sup> Calculated values and the anatase contents decrease in the following order: 40 wt%TiO<sub>2</sub>-ZrO<sub>2</sub> (73.1%) > 60 wt%TiO<sub>2</sub>-ZrO<sub>2</sub> (26.4%) > 20 wt%TiO<sub>2</sub>-ZrO<sub>2</sub> (20%) > 80 wt% TiO<sub>2</sub>-ZrO<sub>2</sub> (13.4%). The order of anatase content is exactly corresponded with the removal efficiency of MO.

#### 4. Conclusions

From the study on the phase transformation and photocatalytic activity of TiO<sub>2</sub>-ZrO<sub>2</sub> nano-sized powders synthesized by the sol-gel process, the following results were obtained.

1. In the as-received TiO<sub>2</sub>-ZrO<sub>2</sub> nano-sized powders, nano-sized TiO<sub>2</sub> particles having an amorphous structure adhered to the ZrO<sub>2</sub> surface, and the phenomenon of aggregation was increased as the increase of TiO<sub>2</sub> content increased.

2. In TiO<sub>2</sub>-ZrO<sub>2</sub> nano-sized powders calcined at 450°C, TiO<sub>2</sub> was an anatase type independent of contents. On the other hand, in the TiO<sub>2</sub>-20 wt%ZrO<sub>2</sub> nano-sized powders calcined at 750°C, the anatase to rutile phase transformation increased remarkably while in the TiO<sub>2</sub>-80 wt%ZrO<sub>2</sub> nano-sized powders, it was retarded.

3. The TiO<sub>2</sub>-40 wt%ZrO<sub>2</sub> and TiO<sub>2</sub>-20 wt%ZrO<sub>2</sub> nano-sized powders calcined at 450°C showed an excellent efficiency of photocatalytic activity, but in the sample calcined at 750°C, the efficiency of MO decomposition was reduced due to the appearance of the rutile type, having a low efficiency of photocatalytic activity.

### Acknowledgements

This work was supported by NRL research program of the Korean Ministry of Science and Technology.

### REFERENCES

1. K. I. Ishibashi, A. Fujishima, T. Watanabe, and K. Hashimoto, "Quantum Yields of Active Oxidative Species Formed on TiO<sub>2</sub> Photocatalyst," *J. Photochem. Photobiol.*, **A134** [1-2] 139-42 (2000).
2. J. C. Yu, J. Yu, L. Zhang, and W. Ho, "Enhancing Effects of Water Content and Ultrasonic Irradiation on the Photocatalytic Activity of Nano-Sized TiO<sub>2</sub> Powders," *J. Photochem. Photobiol.*, **A148** 263-71 (2002).
3. M. Inagaki, Y. Nakazawa, M. Hirano, Y. Kobayashi, and M. Toyoda, "Preparation of Stable Anatase-Type TiO<sub>2</sub> and Its Photocatalytic Performance," *Int. J. Inorg. Mater.*, **3** 809-11 (2001).
4. S. Ruan, F. Wu, T. Zhang, W. Gao, B. Xu, and M. Zhao, "Surface State Studies of TiO<sub>2</sub> Nanoparticles and Photocatalytic Degradation of Methyl Orange in Aqueous TiO<sub>2</sub> Dispersions," *Mater. Chem. Phys.*, **69** 7-9 (2001).
5. J. Chen, D. F. Ollis, W. H. Rulkens, and H. Bruning, "Photocatalyzed Oxidation of Alcohols and Organochlorides in the Presence of Native TiO<sub>2</sub> and Metallized TiO<sub>2</sub> Suspensions. Part (I): Photocatalytic Activity and pH Influence," *Wat. Res.*, **33** [3] 661-68 (1999).
6. V. Loddo, G. Marci, C. Martín, L. Palmisano, V. Rives, and A. Scalfani, "Preparation and Characterisation of TiO<sub>2</sub> (Anatase) Supported on TiO<sub>2</sub> (Rutile) Catalysts Employed for 4-Nitrophenol Photodegradation in Aqueous Medium and Comparison with TiO<sub>2</sub> (Anatase) Supported on Al<sub>2</sub>O<sub>3</sub>," *Appl. Catal.*, **B20** 29-45 (1999).
7. J. Lichtenberger and M. D. Amiridis, "Catalytic Oxidation of Chlorinated Benzenes Over V<sub>2</sub>O<sub>5</sub>/TiO<sub>2</sub> Catalysts," *J. Catal.*, **223** [2] 296-308 (2004).
8. X. Z. Li, F. B. Li, C. L. Yang, and W. K. G, "Photocatalytic Activity of WO<sub>3</sub>-TiO<sub>2</sub> under Visible Light Irradiation," *J. Photochem. Photobiol.*, **A141** 209-17 (2001).
9. D. Das, H. K. Mishra, K. M. Parida, and A. K. Dalai, "Preparation, Physico-Chemical Characterization and Catalytic Activity of Sulphated ZrO<sub>2</sub>TiO<sub>2</sub> Mixed Oxides," *J. Mol. Catal.*, **A189** 271-82 (2002).
10. M. Hirano, C. Nakahara, K. Ota, O. Tanaike, and M. Inagaki, "Photoactivity and Phase Stability of ZrO<sub>2</sub>-Doped Anatase-Type TiO<sub>2</sub> Directly Formed as Nanometer-Sized Particles by Hydrolysis under Hydrothermal Conditions," *J. Solid State Chem.*, **170** 39-47 (2003).
11. L. Shi, C. Li, A. Chen, Y. Zhu, and D. Fang, "Morphology and Structure of Nanosized TiO<sub>2</sub> Particles Synthesized by Gas-Phase Reaction," *Mater. Chem. Phys.*, **66** 51-7 (2000).
12. M. Inagaki, Y. Nakazawa, M. Hirano, Y. Kobayashi, and M. Toyoda, "Preparation of Stable Anatase-Type TiO<sub>2</sub> and Its Photocatalytic Performance," *Int. J. Inorg. Mater.*, **3** 809-11 (2001).
13. D. Byun, Y. Jin, B. Kim, J. K. Lee, and D. Park, "Photocatalytic TiO<sub>2</sub> Deposition by Chemical Vapor Deposition," *J. Haz. Mater.*, **B73** 199-206 (2000).
14. J. C. Yu, H. Y. Tang, J. Yu, H. C. Chan, L. Zhang, Y. Xie, H. Wang, and S. P. Wong, "Bactericidal and Photocatalytic Activities of TiO<sub>2</sub> Thin Films Prepared by Sol-Gel and Reverse Micelle Methods," *J. Photochem. Photobiol.*, **A153** 211-19 (2002).
15. B. Li, X. Wang, M. Yan, and L. Li, "Preparation and Characterization of Nano-TiO<sub>2</sub> Powder," *Mater. Chem. Phys.*, **78** 184-88 (2002).
16. T. Klimova, M. L. Rojas, P. Castillo, R. Cuevas, and J. Ramirez, "Characterization of Al<sub>2</sub>O<sub>3</sub>-ZrO<sub>2</sub> Mixed Oxide Catalytic Supports Prepared by the Sol-Gel Method," *Micropor. Mesopor. Mater.*, **20** 293-306 (1998).
17. J. K. Han, F. Saito, and B. T. Lee, "Microstructures of Porous Al<sub>2</sub>O<sub>3</sub>-50 wt%ZrO<sub>2</sub> Composites Using In-Situ Synthesized Al<sub>2</sub>O<sub>3</sub>-ZrO<sub>2</sub> Composite Powders," *Mater. Lett.*, **58** 2181-85 (2004).
18. J. K. Han, S. M. Choi, I. H. Oh, F. Saito, and B. T. Lee, "Photocatalysis for Oxidation of Phenol and Reduction of Inorganic Pollutants by Nanocrystalline TiO<sub>2</sub>-ZrO<sub>2</sub> Powders," *Mat. Sci. Forum*, **449-452** 289-92 (2004).
19. D. L. Pavia, G. M. Lampman, and G. S. Kriz, "Introduction to Spectroscopy: A Guide for Students of Organic Chemistry," pp. 205-13 Edited by Sanders Golden Sunburst Series (1996).
20. J. Yang and J. M. F. Ferreira, "On the Titania Phase Transition by Zirconia Additive in a Sol-Gel Derived Powder," *Mater. Res. Bull.*, **33** [3] 389-94 (1998).